extending 2 kb on either side of miRNA166 were identified from GenBank by BLAST analyses. Pairwise comparisons between *MIR166* genes were made using Pustell DNA matrix analysis (MacVector 6.5.3). GenBank accession numbers are: *rld1*, AY501430; *mir166a*, AY501431; *mir166b*, AY501432; *mir166c*, AY501433; *mir166d*, AY501434.

In situ hybridization

Tissue sections prepared from shoot apices of two-week-old mutant and wild-type seedlings were pretreated and hybridized as described[27]. Digoxigenin-labelled probes were prepared by *in vitro* transcription (Stratagene) according to the manufacturer's protocol. An *rld1*-specific probe encompassing nucleotides 619–1,674 of the coding sequence, and a *phb*-specific probe encompassing amino acids 462–606 of the *Arabidopsis* PHB protein were used at a concentration of 0.5 ng μl^{-1} kb^{-1} probe complexity. miRNA166 expression was determined using a *mir166a*-derived probe amplified with primers 6F and 7R. A precursor-specific probe was amplified using primer 7R and a gene-specific primer (CCTCCATCAGATGAGCTCC) downstream of miRNA166.

Received 4 December 2003; accepted 23 January 2004; doi:10.1038/nature02363.

1. Carrington, J. C. & Ambros, V. Role of microRNAs in plant and animal development. *Science* **301,** 336–338 (2003).
2. McConnell, J. R. *et al.* Role of *PHABULOSA* and *PHAVOLUTA* in determining radial patterning in shoots. *Nature* **411,** 709–713 (2001).
3. Emery, J. F. *et al.* Radial patterning of *Arabidopsis* shoots by class III *HD-ZIP* and *KANADI* genes. *Curr. Biol.* **13,** 1768–1774 (2003).
4. Otsuga, D., DeGuzman, B., Prigge, M. J., Drews, G. N. & Clark, S. E. *REVOLUTA* regulates meristem initiation at lateral positions. *Plant J.* **25,** 223–236 (2001).
5. Eshed, Y., Baum, S. F., Perea, J. V. & Bowman, J. L. Establishment of polarity in lateral organs of plants. *Curr. Biol.* **11,** 1251–1260 (2001).
6. Kerstetter, R. A., Bollman, K., Taylor, R. A., Bomblies, K. & Poethig, R. S. *KANADI* regulates organ polarity in *Arabidopsis*. *Nature* **411,** 706–709 (2001).
7. Sawa, S. *et al. FILAMENTOUS FLOWER*, a meristem and organ identity gene of *Arabidopsis*, encodes a protein with a zinc finger and HMG-related domains. *Genes Dev.* **13,** 1079–1088 (1999).
8. Siegfried, K. R. *et al.* Members of the *YABBY* gene family specify abaxial cell fate in *Arabidopsis*. *Development* **126,** 4117–4128 (1999).
9. Reinhart, B. J., Weinstein, E. G., Rhoades, M. W., Bartel, B. & Bartel, D. P. MicroRNAs in plants. *Genes Dev.* **16,** 1616–1626 (2002).
10. Rhoades, M. W. *et al.* Prediction of plant microRNA targets. *Cell* **110,** 513–520 (2002).
11. Tang, G., Reinhart, B. J., Bartel, D. P. & Zamore, P. D. A biochemical framework for RNA silencing in plants. *Genes Dev.* **17,** 49–63 (2003).
12. McConnell, J. R. & Barton, M. K. Leaf polarity and meristem formation in *Arabidopsis*. *Development* **125,** 2935–2942 (1998).
13. Nelson, J. M., Lane, B. & Freeling, M. Expression of a mutant maize gene in the ventral leaf epidermis is sufficient to signal a switch of the leaf's dorsoventral axis. *Development* **129,** 4581–4589 (2002).
14. Llave, C., Kasschau, K. D., Rector, M. A. & Carrington, J. C. Endogenous and silencing-associated small RNAs in plants. *Plant Cell* **14,** 1605–1619 (2002).
15. Park, W., Li, J., Song, R., Messing, J. & Chen, X. CARPEL FACTORY, a Dicer homolog, and HEN1, a novel protein, act in microRNA metabolism in *Arabidopsis thaliana*. *Curr. Biol.* **12,** 1484–1495 (2002).
16. Aukerman, M. J. & Sakai, H. Regulation of flowering time and floral organ identity by a microRNA and its *APETALA2*-like target genes. *Plant Cell* **15,** 2730–2741 (2003).
17. Palatnik, J. F. *et al.* Control of leaf morphogenesis by microRNAs. *Nature* **425,** 257–263 (2003).
18. Zhong, R. & Ye, Z. H. *IFL1*, a gene regulating interfascicular fiber differentiation in *Arabidopsis*, encodes a homeodomain-leucine zipper protein. *Plant Cell* **11,** 2139–2152 (1999).
19. Ratcliffe, O. J., Riechmann, J. L. & Zhang, J. Z. *INTERFASCICULAR FIBERLESS1* is the same gene as *REVOLUTA*. *Plant Cell* **12,** 315–317 (2000).
20. Llave, C., Xie, Z., Kasschau, K. D. & Carrington, J. C. Cleavage of *Scarecrow-like* mRNA targets directed by a class of *Arabidopsis* miRNA. *Science* **297,** 2053–2056 (2002).
21. Timmermans, M. C. P., Schultes, N. P., Jankovsky, J. P. & Nelson, T. *Leafbladeless1* is required for dorsoventrality of lateral organs in maize. *Development* **125,** 2813–2823 (1998).
22. Sussex, I. M. Morphogenesis in *Solanum tuberosum* L.: Experimental investigation of leaf dorsiventrality and orientation in the juvenile shoot. *Phytomorphology* **5,** 286–300 (1955).
23. Snow, M. & Snow, R. The dorsiventrality of leaf primordia. *New Phytol.* **58,** 188–207 (1959).
24. Foster, T. M. *et al.* A surveillance system regulates selective entry of RNA into the shoot apex. *Plant Cell* **14,** 1479–1508 (2002).
25. Burr, B., Burr, F. A., Thompson, K. H., Albertson, M. C. & Stuber, C. W. Gene mapping with recombinant inbreds in maize. *Genetics* **118,** 519–526 (1988).
26. Timmermans, M. C. P., Das, O. P. & Messing, J. Characterization of a meiotic crossover in maize identified by a restriction fragment length polymorphism-based method. *Genetics* **143,** 1771–1783 (1996).
27. Jackson, D. in *Molecular Plant Pathology: A Practical Approach* (eds Bowles, D. J., Gurr, S. J. & McPherson, M.) 163–174 (Oxford Univ. Press, Oxford, 1991).

Acknowledgements We thank T. Phelps-Durr, C. Kidner, T. Volpe and G. Hannon for discussions and comments on the manuscript. We also thank T. Mulligan for plant care. This work was supported by grants from the USDA. and the NSF (to M.C.P.T.). M.T.J. is funded in part by a W. Burghardt Turner Fellowship, and J.S.K. is an Alfred Hershey Fellow of the Watson School of Biological Sciences and is supported by a grant from the National Institute of General Medical Sciences, NIH.

Competing interests statement The authors declare that they have no competing financial interests.

Correspondence and requests for materials should be addressed to M.C.P.T. (timmerma@cshl.org).

A non-B-DNA structure at the *Bcl-2* major breakpoint region is cleaved by the RAG complex

Sathees C. Raghavan[1,2], Patrick C. Swanson[6], Xiantuo Wu[1], Chih-Lin Hsieh[1,3,4] & Michael R. Lieber[1,2,3,5]

[1]*Norris Comprehensive Cancer Center, Room 5428,* [2]*Departments of Pathology,* [3]*Biochemistry & Molecular Biology,* [4]*Urology,* [5]*Biological Science and Molecular Microbiology & Immunology, University of Southern California Keck School of Medicine, 1441 Eastlake Ave., MC9176, Los Angeles, California 90033, USA*
[6]*Department of Medical Microbiology and Immunology, Creighton University School of Medicine, 2500 California Plaza, Omaha, Nebraska 68178, USA*

The causes of spontaneous chromosomal translocations in somatic cells of biological organisms are largely unknown, although double-strand DNA breaks are required in all proposed mechanisms[1–5]. The most common chromosomal abnormality in human cancer is the reciprocal translocation between chromosomes 14 and 18 (t(14;18)), which occurs in follicular lymphomas. The break at the immunoglobulin heavy-chain locus on chromosome 14 is an interruption of the normal V(D)J recombination process. But the breakage on chromosome 18, at the *Bcl-2* gene, occurs within a confined 150-base-pair region (the major breakpoint region or Mbr) for reasons that have remained enigmatic. We have reproduced key features of the translocation process on an episome that propagates in human cells. The RAG complex—which is the normal enzyme for DNA cleavage at V, D or J segments—nicks the *Bcl-2* Mbr *in vitro* and *in vivo* in a manner that reflects the pattern of the chromosomal translocations; however, the Mbr is not a V(D)J recombination signal. Rather the *Bcl-2* Mbr assumes a non-B-form DNA structure within the chromosomes of human cells at 20–30% of alleles. Purified DNA assuming this structure contains stable regions of single-strandedness, which correspond well to the translocation regions in patients. Hence, a stable non-B-DNA structure in the human genome appears to be the basis for the fragility of the *Bcl-2* Mbr, and the RAG complex is able to cleave this structure.

The RAG complex can misrecognize and cleave pseudo-signals at lymphoid translocation breakpoints at LMO2, Ttg-1 and SIL[6]. We tested the RAG-misrecognition hypothesis at the *Bcl-2* Mbr, although there is no apparent V(D)J heptamer/nonamer sequence within it (Supplementary Fig. 1). To test whether the *Bcl-2* sequence serves as a recombination signal, a 300-base-pair (bp) *Bcl-2* sequence (containing the 150-bp Mbr region) was positioned 250-bp upstream or downstream of a single 12- or 23-signal sequence on an episome that can replicate in human cells. We transfected the substrates into the human pre-B-cell line Reh, and recovered them 48 h later (Supplementary Fig. 2).

The boundaries of the recovered recombinant molecules were characterized. None of the breakpoint boundaries was at the 12- or 23-signals; rather, the recombinants were far to one side or the other of each signal and clearly not related to V(D)J recombination. However, a disproportionate number of recombination boundaries were in the *Bcl-2* Mbr (Table 1). The recombination frequency (0.056%) was 160-fold lower in our constructs than in a substrate with a pair of optimal 12/23-signals (recombination frequency, 9%) in Reh cells. The pattern of the recombination breakpoints within the *Bcl-2* Mbr was striking. About 77% (27 out of 35) of the breakpoints were within the Mbr, and another five of the 35 events were immediately outside (within five to seven nucleotides) of the *Bcl-2* Mbr (Table 1). Interestingly, most of these 27 events were within peaks I, II or III of the Mbr (data not shown). The difference between the 77% in the Mbr versus the expected random level of

Table 1 **Breakpoint frequencies in plasmids from cells expressing RAG proteins**

	DA	DAC_{Total}			$(DAC_{Mbr}/DA) \times 100$	% Events inside Mbr	% Events outside Mbr
		DAC_{23}	DAC_{Mbr}	$DAC_{Not\ Mbr}$			
Reh	48,250	0	27	8	5.6×10^{-2}	77.0% (27/35)*	23.0% (8/35)
293 + RAGs	616,100	0	26	8	4.2×10^{-3}	76.5% (26/34)*	23.5% (8/34)
293	1,148,300	0	14	19	1.2×10^{-3}	42.4% (14/33)*	57.6% (19/33)
293 + Mut RAGs	274,300	0	3	5	1.1×10^{-3}	37.5% (3/8)	62.5% (5/8)
Random distribution	–	–	–	–	–	48.0%	52.0%

The episome (pXW5) was transfected into mammalian cells (either Reh or 293T cells with or without RAG constructs). The DNA was harvested by the rapid alkaline lysis method after 48 h (Reh) or 40 h (293T), and the recombinants were selected on ampicillin–chloramphenicol plates after transformation into *Escherichia coli*. Plasmid DNA was further screened by restriction digestion (*Sal*I/*Bgl*II) to select clones containing breakpoints at the *Bcl-2* region (inside Mbr, 150 bp or outside Mbr, 160 bp) and sequenced. The number of replicated molecules is indicated as DA, which stands for *Dpn*I-resistant, ampicillin resistant. DAC_{Total} indicates the total number of ampicillin–chloramphenicol double-resistant transformants (recombinants) obtained. Of this group, DAC_{23} are recombinants that use the 23-signal sequence for recombination (zero here). DAC_{Mbr} are recombinants with a breakpoint at *Bcl-2* Mbr. $DAC_{Not\ Mbr}$ is the recombinants with breakpoints at a 160-bp region that is outside the Mbr. The recombination efficiency of Mbr is calculated by dividing DAC_{Mbr} by DA. The frequency of recombinants obtained is indicated as a percentage (% Events). Actual numbers of recombinant clones obtained of a given type (divided by the total recombinants) are indicated in parentheses. Reh indicates recombinants obtained from Reh cells (which have native RAGs); 293 + RAGs indicates that the cells were also transfected with core RAG expression vectors; 293 indicates that the cells were not transfected with RAG vectors; and 293 + Mut RAGs indicates that cells were also transfected with a mutant RAG expression vector. The statistical analysis used the Fisher's exact test.
*$P = 0.006$ for a comparison of the values in rows one and three and in rows two and three of '% Events inside Mbr' column.

48% is highly significant ($P < 0.006$). T-nucleotides (templated nucleotides) were also present at the junctions of these recombinants, a signature feature of t(14;18) in patients (data not shown)[7].

Given that Reh cells have high endogenous levels of RAG proteins, we wondered whether the *Bcl-2* Mbr breaks are caused by RAGs. To test the *in vivo* contribution of RAG proteins to Mbr recombination, we used the human cell line 293T, which does not carry out any detectable V(D)J recombination. We transfected this cell line with a plasmid (pXW5) bearing the *Bcl-2* Mbr (paired with a single 23-signal) with or without RAG1 and RAG2 expression vectors or with mutant RAG1 and RAG2 expression vectors[8,9]. We observed that the recombination frequencies are consistently about three- to fourfold higher in the cells transfected with RAGs than in those without RAGs or with mutant RAGs (Table 1). The recombi-

a

Transfected cells	DA	Total DAC	Boundaries of recombinants: Left DAC_{Mbr}	Left $DAC_{Not\ Mbr}$	Right DAC_{23}	Right $DAC_{Not\ 23}$	$(DAC_{Mbr}/DA) \times 100$	$(DAC_{23}/DA) \times 100$	% Events inside Mbr	% Events outside Mbr
293	1.5×10^6	12	3	9	0	12	2.0×10^{-4}	$< 6.7 \times 10^{-5}$	25.0%	75.0%
293 + RAGs	1.9×10^6	29	24	5	15	14	13×10^{-4}	79×10^{-5}	82.8%	17.2%
293 + Mut RAGs	1.4×10^6	8	3	5	1*	7	2.1×10^{-4}	7.1×10^{-5}	37.5%	62.5%

b

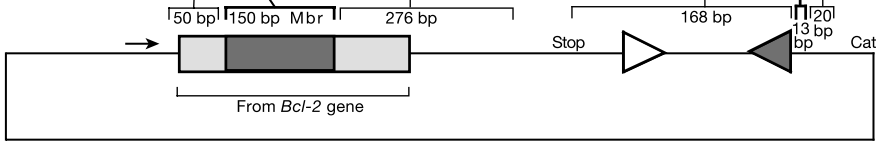

Figure 1 *In vivo* breakpoints on an extrachromosomal substrate cluster within the *Bcl-2* Mbr and are dependent on the RAG complex. The episome (pSCR45) was transfected into mammalian cells (293T cells), recovered 40 h later and analysed in bacteria as described in the Methods. **a**, Comparison of breakpoint frequencies in recombinant plasmid molecules. DA, the number of substrate molecules that replicated in the 293T cells. Total DAC, bacterial transformants that are ampicillin–chloramphenical (double) resistant (also referred to as recombinants). The total DAC for each row is subdivided according to the left and right boundaries of recombination. For the left boundary, DAC_{Mbr} is the subset of double-resistant recombinants that have a breakpoint within the *Bcl-2* Mbr. $DAC_{Not\ Mbr}$ is the subset of recombinants with breakpoints anywhere within the 326-bp region upstream or downstream of the Mbr. For the right boundary, DAC_{23} are recombinants that use the 23-signal sequence for recombination. $DAC_{Not\ 23}$ are recombinants that do not use the 23-signal for recombination. $(DAC_{Mbr}/DA) \times 100$ is the recombination frequency for all events that use the Mbr. $(DAC_{23}/DA) \times 100$ is the recombination frequency for all events that use the 23-signal. The frequency of recombinants obtained is indicated as a percentage (% Events). The row labelled 293 indicates recombinants obtained from 293T cells in the absence of RAGs; 293 + RAGs indicates that cells were also transfected with full-length RAG expression vectors; and 293 + Mut RAGs indicates that the cells were transfected with mutant RAG1 and full-length RAG-2 vectors. The asterisk indicates that this single event may represent a random break that just happens to be within the 13-bp region adjacent to the heptamer of the 23-signal[8]. **b**, Regions of recombination relative to the sequence of pSCR45. The Mbr region is shown in dark grey. The light grey regions are outside of the Mbr but are the flanking regions that naturally are adjacent to the Mbr in the human chromosome. The 12-signal is indicated by the open triangle, and the 23-signal by the filled triangle. The transcriptional promoter (short arrow upstream of the Mbr), the transcription terminator (Stop) and the chloramphenicol gene (Cat) are indicated.

nation frequency of pXW5 (0.004%) in the presence of RAGs is about 25-fold lower than that of a substrate with a pair of optimal 12/23-signals (recombination frequency of 0.1% in fibroblasts transfected with RAG vectors[9]). More importantly, the distribution of the breakpoints was markedly influenced by the presence of the RAG proteins. With RAGs, the breaks were predominantly within the *Bcl-2* Mbr, with particular predilection for peaks I, II and III (76.5%, 26 out of 34 events) (Table 1).

We observed clustering of breaks at the *Bcl-2* Mbr side of the deletion events, but the other boundary of the deletions (recombinants) above were not at the 23-signal. In clinical cases of the *Bcl-2* translocation, breaks at the immunoglobulin heavy chain occur during attempted rearrangement between D and J elements that use 12- and 23-signals (Supplementary Fig. 1). Therefore, we designed a substrate to check the recombination efficiency of the *Bcl-2* Mbr when both the 12- and 23-signals are present rather than one alone (Fig. 1). This plasmid, pSCR45, was then transfected into 293T cells with and without human full-length RAG expression vectors, or with a mutant RAG1 vector[10].

In common with the observations described above for one-signal substrates (Table 1), double-signal substrates have a breakpoint distribution that is strikingly dependent on the Mbr (24 out of 29 events) (Fig. 1a). The preference for breaks in the Mbr occurs despite twice as much DNA surrounding the area where breaks could occur (150 bp in the Mbr compared with 326 bp both upstream and downstream). In more than half of the events (15 out of 29), the second break is at the 23-signal, such that the coding end formerly attached to that signal is now joined to the *Bcl*-2 Mbr break. Such a precise use of the 23-signal only in the simultaneous presence of a 12-signal clearly indicates the involvement of the RAG complex. The presence of both a 12- and a 23-signal permits a recapitulation of the D to J joining process, whereas a single signal does not (Table 1; see also Supplementary Fig. 2). This indicates that the *Bcl-2* Mbr recombination with the coding end of the 23-signal is likely to be an interruption of the normal 12/23-recombination. In the absence of RAGs or with mutant RAGs, there is little or no cleavage at the 23-signal (Fig. 1a).

Given that the *Bcl-2* Mbr recombined with a coding end adjacent to a 23-signal, the involvement of the RAG proteins is clear. But if the RAG complex recombines the Mbr *in vivo*, is it possible that it might cleave the Mbr in a purified system consisting only of the RAG complex and the Mbr DNA? To test this, we incubated the *Bcl-2*-Mbr-bearing plasmids with the purified RAG complex under standard physiological divalent cation (Mg^{2+}) buffer conditions for RAG cleavage reactions. Although the core and full-length RAG complexes do not nick the top strand of the Mbr, they consistently nick the bottom strand to an extent that is similar to its nicking of a standard 23-signal (Supplementary Fig. 3). Active-site mutant RAGs and controls (which do not have RAGs) showed no nicking (see Supplementary text).

These *in vitro* nicking results by RAGs are consistent with the *in vivo* substrate recombination. However, what feature of the Mbr does the RAG complex recognize if the Mbr does not function as a recombination signal?

In the absence of any heptamer/nonamer function by the *Bcl-2* Mbr, we wondered whether there is a structural basis for the fragility at this 150-bp region. To test for single-strandedness of the *Bcl-2* Mbr, we used chemical-probing methods on genomic DNA[11,12]. To study the single-strandedness of chromosomal DNA at the single-molecule level, bisulphite-treated DNA is polymerase chain reaction (PCR)-amplified, cloned and sequenced. Bisulphite converts unpaired cytosines to uracil, and these become thymine after PCR amplification, thus allowing the detection of single-stranded regions[11].

The chromosomal DNA extracted from Reh cells was used for bisulphite treatment. A PCR fragment of 528 bp containing the *Bcl-2* Mbr amplified from treated DNA was cloned, sequenced and analysed. Most cytosine conversions occur in peaks I and III of the Mbr region (Fig. 2). If we display the results for individual strands,

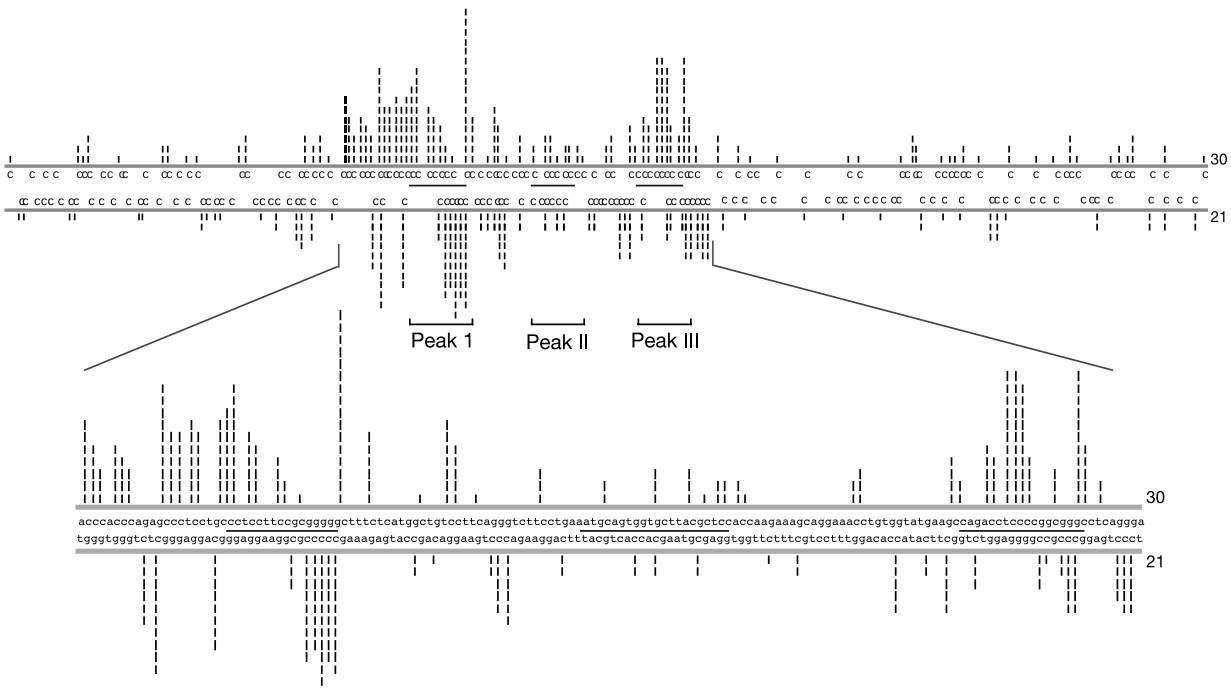

Figure 2 Bisulphite reactivity at the *Bcl-2* Mbr on chromosomal DNA. A 528-bp fragment containing the Mbr amplified from chromosomal DNA after bisulphite treatment is shown. The 150-bp *Bcl-2* Mbr region is expanded to show the complete sequence. The three breakpoint peaks are indicated by three short horizontal lines between the top and bottom strands (see Supplementary Fig. 1). Bisulphite sensitivity is shown for the 250 bp downstream of the Mbr and 125 bp upstream of the Mbr. Vertical incremental bars (vertical dashes) above the line indicate the sensitivity for the top strand, and bars below the line indicate the sensitivity for the bottom strand; each vertical bar represents a cytosine conversion on one molecule. The total numbers of molecules sequenced from the top and bottom strands are indicated at the right margin.

we find that 28% of human chromosomal alleles have long single-stranded regions at peaks I and III of the *Bcl-2* Mbr. (Overall 15.5% of the cytosines are converted; Fig. 3.) There is also a tendency for consecutive cytosines to be converted (seven or more cytosine residues distributed over 14–49 bp) (Figs 2 and 3). These regions of single-strandedness suggest the existence of a non-B-form single-stranded DNA conformation at the Mbr in this human pre-B-cell line.

Controls at nine unrelated genomic sites showed that the *Bcl-2* Mbr is distinctive for the lengths of DNA that are single-stranded (see Supplementary text and Supplementary Fig. 5). We confirmed the single-stranded character of the *Bcl-2* Mbr in chromatin by diffusing two other types of chemical probes ($KMnO_4$ and OsO_4) into viable cells. Results from these experiments also indicated that there is a single-stranded character at the Mbr (see Supplementary text and Supplementary Fig. 6).

To further investigate the requirements of non-B-DNA structure formation at the *Bcl-2* Mbr, plasmid pXW5, bearing the *Bcl-2* fragment, was propagated as a replicating human minichromosome in Reh cells, harvested 42 h later and subjected to the bisulphite modification assay. The results are indistinguishable from those observed above for the chromosomal DNA (see Supplementary Fig. 7). This indicates that, on an episome, the 300-bp region containing the *Bcl-2* Mbr is sufficient to assume the single-stranded conformation that is observed in the human chromosome, regardless of the sequence of the neighbouring regions. Again both B-form and non-B-form conformations exist among the population of molecules and in a similar proportion to that observed in the chromosome (Figs 2 and 3).

We wondered whether plasmid DNA bearing the *Bcl-2* Mbr and harvested from bacteria would be able to form the non-B-DNA structure. pXW5 DNA was extracted using a non-denaturing method and subjected to the bisulphite modification assay. The results obtained after sequencing a 930-bp fragment show a high bisulphite sensitivity in the *Bcl-2* Mbr (Fig. 4a). The single-stranded regions are restricted to peaks I and III (Fig. 4a, c, d), which is the case for the human chromosomal and minichromosomal studies of the same DNA region. The conversion frequency at the *Bcl-2* Mbr is 22.5% when the plasmid DNA is supercoiled, and this is 3.9-fold higher than the background. The Mbr in linearized plasmids is still hyper-reactive with bisulphite relative to the surrounding DNA, although the overall reactivity is reduced by 1.8-fold (Fig. 4b).

PCR fragments of shorter length are able to reproduce the non-B conformation based on the bisulphite reactivity, gel mobility shift and by P1-sensitivity analysis (see Supplementary text).

We have reproduced key aspects of the t(14;18) translocation on

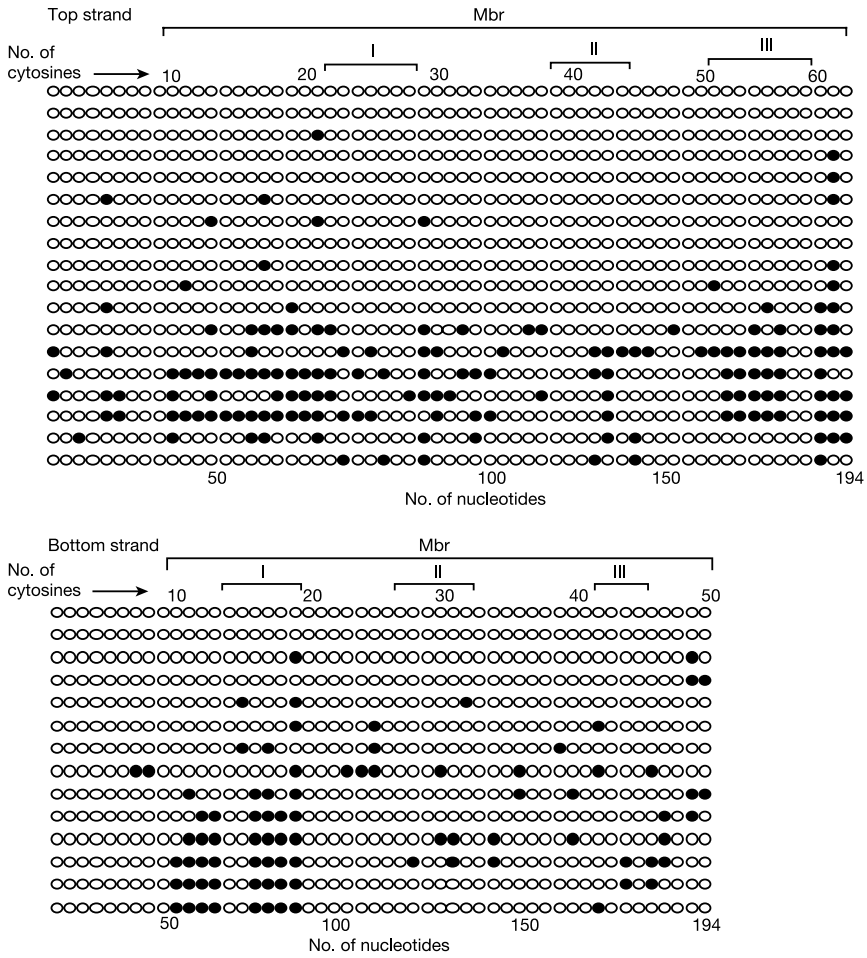

Figure 3 The bimodal nature (B-form DNA versus non-B-form) of the structural configuration of chromosomal DNA at the Mbr. The upper panel shows bisulphite sensitivity of molecules from the top strand, whereas the lower panel shows the corresponding bottom strand data. In both panels, each row of circles represents one DNA molecule. Each filled circle represents an instance of a bisulphite-converted cytosine (single-stranded), whereas open circles represent cytosines resistant to bisulphite (that is, double-stranded DNA). Note that only the C residues are depicted, but a scale to relate the length along the DNA is shown at the bottom. The designations I, II or III correspond to the three translocation frequency peaks within the Mbr. The population of molecules includes a mixture of those that are B-form and those that have substantial focal and recurring regions of single-strandedness (non-B-form).

extrachromosomal DNA substrates transfected into human lymphoid cells. On substrates bearing the *Bcl-2* Mbr and only one of either the 12- or 23-signal, no *in vivo* recombinants using the 12- or 23-signal were detected, even though breaks at the Mbr were quite focused. However, when we included a pair of 12- and 23-signals, Mbr recombination specific to the 23-signal was readily detectable. The simplest explanation for this is that one or both of the coding ends are released during a 12/23 paired V(D)J recombination event[13] and simultaneously a break at the *Bcl-2* Mbr is generated by the RAGs. Subsequently, the break at the Mbr is joined to a coding end from the failed V(D)J recombination reaction in ways that are diagrammatically indistinguishable from the t(14;18) translocation (Supplementary Fig. 1a). The Mbr break does not seem to involve direct pairing with any 12- or 23-signal; otherwise, we would have seen recombination on substrates that carry the Mbr and only one signal.

We have noted that the single-strandedness at both peaks I and III varies between individual molecules (Figs 3 and 4). For peak II, there is no marked degree of single-strandedness, and yet it, like peaks I and III, is subject to translocation. We propose that the single strands at peaks I and III interact such that the region between them (peak II) is a site of marked DNA bending. Although the correlation between the single-stranded regions and the translocations is quite good at peaks I and III, there remains the possibility that *in vivo* proteins bound to these single-stranded and adjacent double-stranded regions may modify further the conformations, thereby explaining the lack of single-strandedness at peak II.

Why would the RAG complex cleave the non-B-form DNA structure at the *Bcl-2* Mbr? There are two known structures that the RAG complex has been demonstrated to cleave in a sequence-independent manner, and both have stable single-stranded character, in common with the structure here. First, the RAG complex (and other transposase enzymes) cleaves single-stranded 3′ overhangs in Mg^{2+}-containing buffers[14]. This may reflect some common structural features between 3′ overhangs and the presumed single-strandedness thought to exist at the border of the heptamer, where RAGs normally cleave[15]. Second, the RAG complex opens DNA hairpins in Mn^{2+}-containing buffers[16]. This RAG-mediated hairpin opening is inefficient in Mg^{2+} buffers, and it may not be physiologically relevant to hairpin opening[17], but it illustrates that RAG proteins have some low level of activity on such non-B configurations. Could the non-B-form structure at the *Bcl-2* Mbr somehow be a target for nicking? This appears to be the case, given the efficient nicking at or very near the three peaks of the *Bcl-2* Mbr. We note that we cannot rule out the possibility that any of a number of other structure-specific nucleases contribute to cleavage at the Mbr; however, the low level of focused cleavage in cells that do not express RAGs would argue that other nucleases can only play a minor role, if any at all.

In this study, we have clearly demonstrated that non-B-form

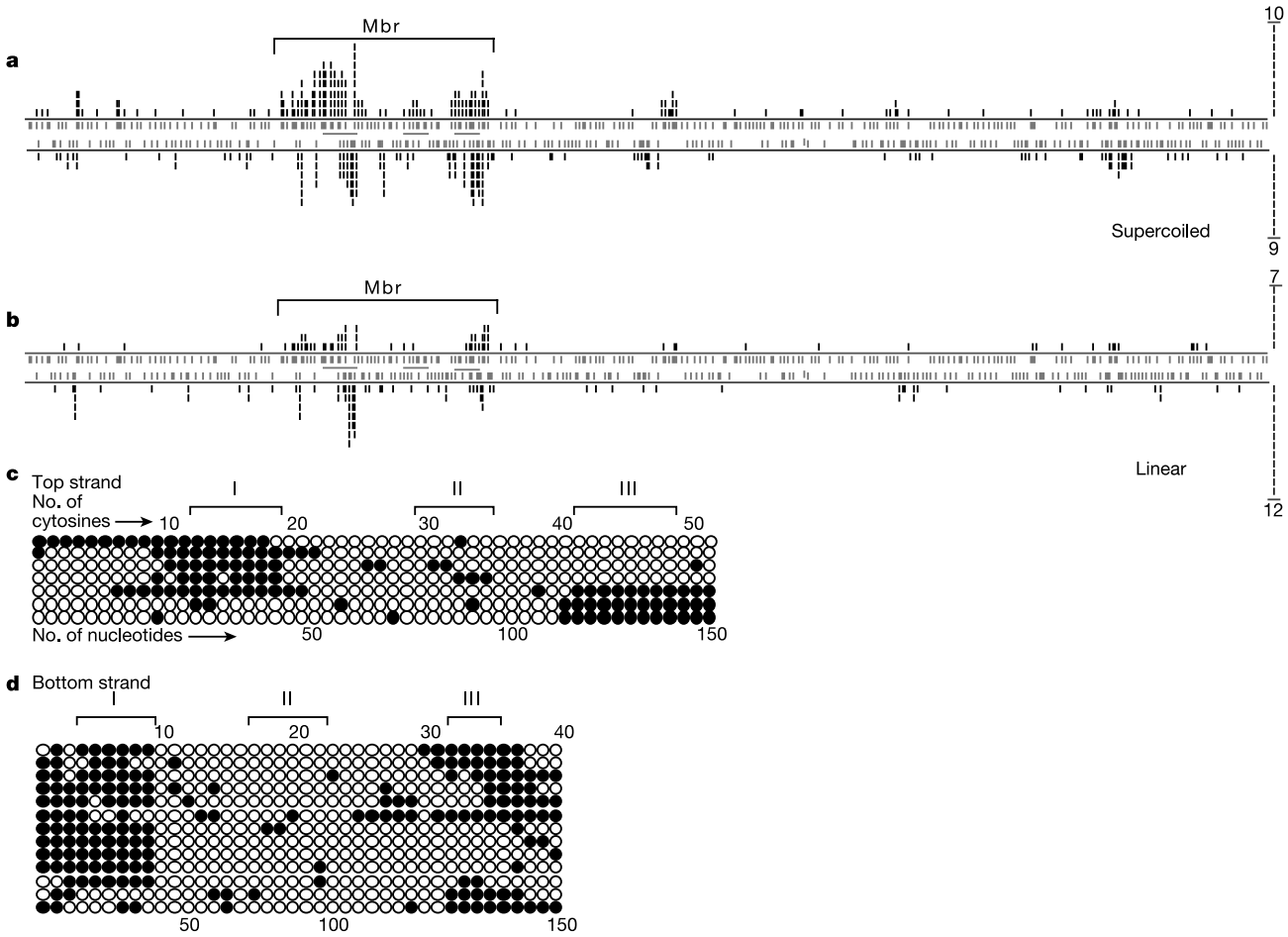

Figure 4 The bisulphite sensitivity of the *Bcl-2* Mbr on plasmid DNA. The pXW5 plasmid DNA was purified from *Escherichia coli* by a non-denaturing method (see Supplementary Methods). Following bisulphite modification, a 930-bp DNA fragment containing the *Bcl-2* Mbr was PCR-amplified and sequenced. **a**, **b**, Supercoiled plasmid DNA (**a**) and linear plasmid DNA (**b**) (linearized by *Bgl* II digestion) is shown. **c**, **d**, Distribution of bisulphite reactivity on molecules with seven or more C to T conversions in a string on the top (**c**) or bottom (**d**) strands of the *Bcl-2* Mbr on supercoiled pXW5. (See Supplementary Fig. 7 legend for more details.)

DNA structural alterations can occur in the human genome and that these alterations can demarcate the precise boundaries of sites of recurrent chromosomal breakage. We have also provided evidence that the RAG complex is responsible for the t(14;18) translocation *in vivo* and *in vitro* and that its role here is different from ones invoked by previously described mechanisms. □

Methods

Plasmid construction and V(D)J recombination assay

The plasmid constructs were made by modifying the SV40-based plasmid, pGG51 (ref. 8). See Supplementary Methods.

Transfection of the 293T cells with pXW5 or pSCR45 along with full-length RAG1/2 (Fig. 1), mutant RAG1/full-length RAG2 (Fig. 1 and Table 1) or core RAG1/2 (Table 1) was done using the calcium-phosphate method as described earlier[9]. The coordinates of the core RAGs are the same as those used for protein production below. Plasmid DNA was alkaline harvested and analysed as described in the Supplementary Methods.

Bisulphite modification assay

The bisulphite modification assay was used as described previously[11] (see Supplementary Methods).

Ligation-mediated PCR

For details of the ligation-mediated PCR see Supplementary Methods.

In vitro RAG nicking assay

Core murine glutathione *S*-transferase (GST)–RAG1 (amino acids 330–1040) and GST–RAG2 (amino acids 1–383), or MBP murine core RAG1 and RAG2, or core RAG1 and full-length MBP RAG2 proteins were overexpressed in the human 293T cells and purified as previously described[10,18]. See Supplementary Methods.

Received 18 October 2003; accepted 19 January 2004; doi:10.1038/nature02355.

1. Lieber, M. R. in *The Causes and Consequences of Chromosomal Aberrations* (ed. Kirsch, I.) 239–275 (CRC Press, Boca Raton, 1993).
2. Lewis, S. M. The mechanism of V(D)J joining: lessons from molecular, immunological and comparative analyses. *Adv. Immunol.* **56,** 27–150 (1994).
3. Dalla-Favera, R. in *The Causes and Consequences of Chromosomal Aberrations* (ed. Kirsch, I. R.) 313–332 (CRC Press, Boca Raton, 1993).
4. Korsmeyer, S. J. Chromosomal translocations in lymphoid malignancies reveal novel proto-oncogenes. *Annu. Rev. Immunol.* **10,** 785–807 (1992).
5. Tycko, B. & Sklar, J. Chromosomal translocations in lymphoid neoplasia: A reappraisal of the recombinase model. *Cancer Cells* **2,** 1–8 (1990).
6. Raghavan, S. C., Kirsch, I. R. & Lieber, M. R. Analysis of the V(D)J recombination efficiency at lymphoid chromosomal translocation breakpoints. *J. Biol. Chem.* **276,** 29126–29133 (2001).
7. Jager, U. *et al.* Follicular lymphomas BCL-2/IgH junctions contain templated nucleotide insertions: novel insights into the mechanism of t(14;18) translocation. *Blood* **95,** 3520–3529 (2000).
8. Gauss, G. H. & Lieber, M. R. Mechanistic constraints on diversity in human V(D)J recombination. *Mol. Cell. Biol.* **16,** 258–269 (1996).
9. Schwarz, K. *et al.* RAG mutations in human B cell-negative SCID. *Science* **274,** 97–99 (1996).
10. Swanson, P. C. The DDE motif in RAG-1 is contributed in trans to a single active site that catalyzes the nicking and transesterification steps of V(D)J recombination. *Mol. Cell. Biol.* **21,** 449–458 (2001).
11. Yu, K., Chedin, F., Hsieh, C.-L., Wilson, T. E. & Lieber, M. R. R-loops at immunoglobulin class switch regions in the chromosomes of stimulated B cells. *Nature Immunol.* **4,** 442–451 (2003).
12. Gough, G. W., Sullivan, K. M. & Lilley, D. M. The structure of cruciforms in supercoiled DNA: probing the single-stranded character of nucleotide bases with bisulphite. *EMBO J.* **5,** 191–196 (1986).
13. Tevelev, A. & Schatz, D. G. Intermolecular V(D)J recombination. *J. Biol. Chem.* **275,** 8341–8348 (2000).
14. Santagata, S. *et al.* The RAG1/RAG2 complex constitutes a 3′ flap endonuclease: implications for junctional diversity in V(D)J and transpositional recombination. *Mol. Cell* **4,** 935–947 (1999).
15. Ramsden, D. A., McBlane, J. F., van Gent, D. C. & Gellert, M. Distinct DNA sequence and structure requirements for the two steps of V(D)J recombination signal cleavage. *EMBO J.* **15,** 3197–3206 (1996).
16. Besmer, E. *et al.* Hairpin coding end opening is mediated by the recombination activating genes RAG1 and RAG2. *Mol. Cell* **2,** 817–828 (1998).
17. Ma, Y., Pannicke, U., Schwarz, K. & Lieber, M. R. Hairpin opening and overhang processing by an Artemis:DNA-PKcs complex in V(D)J recombination and in nonhomologous end joining. *Cell* **108,** 781–794 (2002).
18. Yu, K. & Lieber, M. R. The nicking step of V(D)J recombination is independent of synapsis: implications for the immune repertoire. *Mol. Cell. Biol.* **20,** 7914–7921 (2000).

Supplementary Information accompanies the paper on **www.nature.com/nature**.

Acknowledgements We thank S. J. Korsmeyer for guidance during the early phases of this work. We also thank I. Haworth, J. S. Lee, P. Chastian and D. Shibata for discussions of the work, and NIH for grants to M.R.L.

Competing interests statement The authors declare that they have no competing financial interests.

Correspondence and requests for materials should be addressed to M.R.L. (lieber@usc.edu).

Tension between two kinetochores suffices for their bi-orientation on the mitotic spindle

Hilary Dewar[1], Kozo Tanaka[1], Kim Nasmyth[2] & Tomoyuki U. Tanaka[1]

[1]*School of Life Sciences, University of Dundee, Wellcome Trust Biocentre, Dundee DD1 5EH, UK*
[2]*Research Institute of Molecular Pathology, Dr Bohr-Gasse 7, A-1030 Vienna, Austria*

The movement of sister chromatids to opposite spindle poles during anaphase depends on the prior capture of sister kinetochores by microtubules with opposing orientations (amphitelic attachment or bi-orientation)[1]. In addition to proteins necessary for the kinetochore–microtubule attachment, bi-orientation requires the Ipl1 (Aurora B in animal cells) protein kinase[2–7] and tethering of sister chromatids by cohesin[8,9]. Syntelic attachments, in which sister kinetochores attach to microtubules with the same orientation, must be either 'avoided' or 'corrected'. Avoidance might be facilitated by the juxtaposition of sister kinetochores such that they face in opposite directions; kinetochore geometry is therefore deemed important. Error correction, by contrast, is thought to stem from the stabilization of kinetochore–spindle pole connections by tension in microtubules, kinetochores, or the surrounding chromatin arising from amphitelic but not syntelic attachment[10,11]. The tension model predicts that any type of connection between two kinetochores suffices for efficient bi-orientation. Here we show that the two kinetochores of engineered, unreplicated dicentric chromosomes in *Saccharomyces cerevisiae* bi-orient efficiently, implying that sister kinetochore geometry is dispensable for bi-orientation. We also show that Ipl1 facilitates bi-orientation by promoting the turnover of kinetochore–spindle pole connections in a tension-dependent manner.

Evidence for an error correction mechanism facilitating bi-orientation has been hitherto confined to meiotic cells, where homologous kinetochores are connected by chiasmata, whose remoteness from the sites of microtubule attachment precludes a key role for kinetochore geometry. Thus, in grasshopper spermatocytes whose kinetochores and spindle poles are repeatedly connected and disconnected by microtubules until they bi-orient, the kinetochore-to-pole connections of a 'maternal' chromosome can be stabilized by using a glass needle to pull on the 'paternal' chromosome attached to it[10,11]. If bi-orientation were established in mitotic cells by a similar tension-sensitive error correction mechanism, then any kind of connection between two kinetochores would suffice for their bi-orientation, including two kinetochores situated on the same chromatid. We therefore set out to analyse the behaviour of dicentric minichromosomes that are unable to replicate during S phase.

We addressed this issue in the budding yeast *S. cerevisiae*, whose kinetochores possess only a single microtubule-binding site[12] and whose centromeres (the DNA underlying the kinetochore) have been pinpointed to sequences no longer than 120 base pairs (bp)[13]. Their activity can therefore be turned off by transcription from an adjacent promoter[14]. The behaviour of yeast centromeres can be followed by marking them with bacterial operators bound by repressor proteins fused to green fluorescent protein (GFP)[8,15,16]. Traction caused by 'amphitelic' attachment overwhelms sister chromatid cohesion at centromeres, but not in the flanking sequences, which leads to their precocious separation before onset of anaphase. The tension so created causes centromeric chromatin to unravel, forming 10-nm (beaded nucleosomes) or even thinner fibres.